small
NANO MICRO

Single-Molecule Colocalization Studies Shed Light on the Idea of Fully Emitting versus Dark Single Quantum Dots

*Thomas Pons, Igor L. Medintz, Dorothy Farrell, Xiang Wang, Amy F. Grimes, Douglas S. English, Lorenzo Berti, and Hedi Mattoussi**

In this report the correlation between the solution photoluminescence (PL) quantum yield and the fluorescence emission of individual semiconductor quantum dots (QDs) is investigated. This is done by taking advantage of previously reported enhancement in the macroscopic quantum yield of water-soluble QDs capped with dihydrolipoic acid (DHLA) when self-assembled with polyhistidine-appended proteins, and by using fluorescence coincidence analysis (FCA) to detect the presence of "bright" and "dark" single QDs in solution. This allows for changes in the fraction of the two QD species to be tracked as the PL yield of the solution is progressively altered. The results clearly indicate that in a dispersion of luminescent nanocrystals, "bright" (intermittently emitting) single QDs coexist with "permanently dark" (non-emitting) QDs. Furthermore, the increase in the fraction of emitting QDs accompanies the increase in the PL quantum yield of the solution. These findings support the idea that a dispersion of QDs consists of two optically distinct populations of nanocrystals—one is "bright" while the other is "dark;" and that the relative fraction of these two populations defines the overall PL yield.

Dr. T. Pons,[+] Dr. I. L. Medintz, Dr. D. Farrell,[++] Prof. H. Mattoussi[+++]
US Naval Research Laboratory
Division of Optical Sciences
Washington, DC 20375, USA
E-mail: mattoussi@chem.fsu.edu
Dr. X. Wang, Dr. A. F. Grimes, Prof. D. S. English[++++]
Dept. of Chemistry & Biochemistry
University of Maryland
College Park, MD 20742, USA
Dr. L. Berti
Department of Biochemistry and Molecular Medicine
University of California
Davis School of Medicine
Sacramento, CA 95817, USA
[+] Present address: Laboratoire Physique et Etude des Matériaux, ESPCI-CNRS UMR8213, Ecole de Physique et Chimie Industrielle (ESPCI), 10 rue Vauquelin, 75005 Paris, France
[++] Present address: National Cancer Institute, Building 31, Room 10A52, Bethesda, MD 20892, USA
[+++] Present address: Florida State University, Department of Chemistry and Biochemistry, Tallahassee, FL 32306, USA; E-mail: mattoussi@chem.fsu.edu
[++++] Present address: Department of Chemistry, Wichita State University, 1845 Fairmount, Wichita, KS 67260, USA

DOI: 10.1002/smll.201100802

1. Introduction

Colloidal semiconductor nanocrystals have several properties that distinguish them from their self-assembled counterparts.[1,2] They are grown in solution environment (from individual atoms in a bottom-up approach) by reduction of organometallic precursors.[1,2] One of the most successful routes involves the pyrolysis of organometallic precursors at high temperature and in the presence of strong coordinating solvent(s). It was first applied by Bawendi and co-workers to prepare high-quality nanocrystals of CdSe,[3] and later expanded by other groups to prepare an array of metal and metal oxide nanocrystals.[4–8] As made, these nanocrystals are capped with bifunctional molecules (ligands), which promote their manipulation and processing from solution environments. These ligands also provide electronic passivation of the nanocrystal surfaces. Although the optical absorption of these materials is little affected by the surface passivation, their photo-induced emission, in contrast, can be drastically influenced by the nature of the ligand binding onto the quantum dot (QD) surface, as well as its electronic properties (electron-donating or electron-withdrawing groups). The emission can also be strongly affected by the presence of a wider bandgap overcoating shell (e.g., ZnS on CdSe core).[9,10]

In 1996, Brus, Bawendi, and co-workers reported that individual QDs exhibit intermittent emission when excited with continuous laser signal: photoexcited isolated colloidal QDs generate blinking emission.[11] This blinking behavior consists of two alternating modes of fluorescence. One corresponds to sustained episodes of emission, "ON," with duration τ_{ON}, where rapid absorption and fluorescence cycling take place. The other corresponds to episodes of no fluorescence emission, "OFF," with duration τ_{OFF}, where the QD is essentially dark.[12] In contrast, self-assembled semiconductor nanocrystals do not exhibit this blinking phenomenon. A flurry of studies followed that first report, where a variety of conditions were explored, including changing the nature of the capping ligands, overcoating the native core with a wider-bandgap semiconducting shell, and investigating the effects of laser power and the influence of the matrix in which the QDs were dispersed.[12–15] These studies have cumulatively shown that the shape of the blinking photoluminescence (PL) signal (e.g., the rate of switching between ON and OFF states) depends on the surface properties and the overall quantum yield of the sample. For example, overcoating the native core with other wider-bandgap semiconducting materials, such as ZnS on CdSe cores, tends to increase τ_{ON} and τ_{OFF} periods while reducing the rate of switching between the two sates;[11] the presence of an overcoating shell is also known to enhance the ensemble fluorescence quantum yield (QY). Kuno and coworkers have shown that the probability densities of both on-time and off-time follow an inverse power law with τ, $P(\tau_{ON/OFF}) \propto (\tau_{ON/OFF})^{-m}$. This law is applicable for over more than seven decades in probability density and five decades in time with m = 1.6–1.7.[12,14,16] This power law is largely unaffected by the various parameters discussed above. There is a slight departure from the simple power law behavior of the probability $P(\tau_{ON})$ at the longer tail of τ_{ON}.

It has also been debated whether the actual solution phase (macroscopic) QY is correlated with the blinking profiles of individual QD emissions via a simple linear conversion (e.g., between the frequency of ON events and QY), or if it is defined by the fraction of bright (still blinking) QDs in the solution, with the rest of the nanocrystals being "permanently dark." The latter rationale implies that a higher macroscopic QY would correspond to a larger fraction of single fluorescing QDs, and vice versa. In an early study, Webb and co-workers devised a set of experiments where emitting QDs could be distinguished from their dark counterparts in the same sample.[17] They labeled QDs conjugated to streptavidin (SA-QDs from Invitrogen) with organic dyes and used colocalization to track and distinguish between bright and permanently dark QDs in the sample. The bright fractions were measured by fluorescence coincidence analysis (FCA) and two-photon fluorescence correlation spectroscopy (FCS). The authors reported that indeed larger fractions of emitting QDs were measured for QD dispersions with higher quantum yields. In addition, they found that the intrinsic brightness of individual QDs stayed constant across samples with different QYs but having the same emission profile (same peak wavelength). Furthermore, using FCS they found that increasing the QDs' illuminated dwell time by tenfold did not change the fraction of apparently dark QDs but increased the detected fraction of blinking QDs, suggesting that the dark population does not arise from millisecond blinking.

We have previously reported that hydrophilic ZnS-overcoated CdSe QDs capped with dihydrolipoic acid (DHLA) exhibit a sizable enhancement in their PL yield when conjugated with increasing numbers of polyhistidine-appended proteins (self assembly driven by metal–His affinity, where His represents histidine).[18,19] In this report we follow from Webb's previous results and use our observation of enhanced QD PL yield upon self-assembly with His-appended proteins to investigate the presence of permanently "dark" QDs, and eventually extract a correlation between the solution quantum yield and fraction of individual "bright" QDs in a macroscopic sample. Our findings confirm that "bright" and "permanently dark" QDs coexist in a macroscopic sample. We also observe that the increase in the QY of a solution of self-assembled QD–protein conjugates is accompanied with an increase in the fraction of "bright" QDs, not by an increase in the brightness of single emitting QDs.

2. Methods

2.1. Quantum Dots

We used two sets of luminescent CdSe–ZnS core–shell QDs. Both were synthesized using a step wise reaction of organometallic precursors in a hot coordinating solvent mixture, as previously reported.[3,6,9,10] The first set of QDs with an emission maximum at 590 nm was prepared in our laboratory and made hydrophilic by exchanging the native trioctylphosphine/trioctylphosphine oxide (TOP/TOPO) cap with dihydrolipoic acid (DHLA) ligands.[19,20] This cap exchange strategy provides QDs that are dispersible in basic buffer solutions; in the present set of experiments we used 10 mM sodium tetraborate buffer at pH 8.6. The second set of 605 nm emitting QDs was obtained from Invitrogen (Carlsbad, CA) and are made water-soluble using a proprietary amphiphilic block copolymer coating and further chemically functionalized to display an average between ~5 and 10 streptavidin per QD (www.invitrogen.com). The coupling chemistry used to attach the streptavidin to the QDs is assumed to leave 3 out of the 4 biotin binding sites on each protein available, suggesting an average of 15–30 biotin binding sites per QD.

2.2. QD–Conjugate Preparation

We used two conjugate configurations.

2.2.1. Configuration 1: QD-MBP-His_5/FITC-peptide

These DHLA-QDs were conjugated simultaneously to a maltose binding protein appended with a C-terminal pentahistidine-sequence (MBP-His_5) and a fluorescein isothiocyanate (FITC)-labeled peptide with an N-terminal pentahistidine (His_5-peptide-FITC), relying on direct coordination between the His_n-tag and the Zn-rich QD surface.[18,21–23] The peptide utilized in this study consists of the sequence

small NANO MICRO

Ac–$(His)_5$GL(Aib)VALGGK*–$CONH_2$, where Ac is an acetyl group blocking the N-terminal amine, Aib is the artificial residue α-aminoisobutyric acid (G (glycine), L (leucine), V (valine), A (alanine), K (lysine)), and $CONH_2$ is an amide group blocking the C-terminal carboxyl.[24] The pendant primary amine on the lysine side chain (K*) was labeled with fluorescein-5-isothiocyanate (FITC Isomer I, Invitrogen) by adding an excess of the dye in 0.136 M sodium tetraborate buffer at pH 8.5.[25] FITC-labeled peptide was separated from excess dye via reverse-phase high-performance liquid chromatography (HPLC) on a semipreparative Agilent Zorbax C18, 300 Å (9.4 mm × 250 mm) using as eluents acetonitrile with 0.1% trifluoroacetic acid (TFA) and water with 0.1% TFA at a gradient of 1% acetonitrile/min. The peptide was then quantitated by UV–vis spectroscopy, lyophylized and stored at –20 °C in a dessicator until needed, as described in detail in the literature.[26] For QD bioconjugation, the peptide was resolubilized in the equivalent of 10% of the final volume of dimethylsulfoxide (DMSO) and then brought up to volume in 10 mM borate buffer. QDs were first mixed with His_5-peptide-FITC (at the desired indicated ratios) for several minutes and then MBP-His_5 in 10 mM borate buffer at pH 8.6 and allowed to self-assemble for ~30 min to 1 h prior to analysis. In this mixed surface QD-MBP/peptide conjugation, the average number of peptides was fixed at 3, while that of MBP-His_5 per QD was increased from 0 to 16. This approach assured that the peptide was attached to the QD prior to self-assembly with the MBP-His_5. This approach allowed a progressive increase in the QD–conjugate fluorescence quantum yield while maintaining the overall number of FITC dyes coupled to each QD fixed.

2.2.2. Configuration 2: QD-Streptavidin/TET-DNA Conjugates

In this configuration a dye-labeled and biotinylated DNA was utilized. A synthetic DNA sequence consisting of 5′-[5TET]-AGCTAGCT-[BioTEG-Q]-3′ was obtained from Operon (Huntsville, Texas) where 5TET is the dye 5′-tetrachloro-fluorescein and BioTEG-Q is a biotin displaying a triethylene glycol linker allowing for more efficient binding to streptavidin's deep binding pocket. The QDs were mixed with the indicated ratios of DNA and allowed to self-assemble for at least 1 h in borate buffer prior to analysis. In both cases, the dyes were selected so that they would have absorption far removed from the QD emission, to minimize potential energy transfer interactions with the QDs. **Figure 1** and **2** show the absorption and emission spectra of the QDs and dyes used. Dye samples and bioconjugation reactions were also handled away from direct light sources to minimize any potential photobleaching effects.

2.3. Absorption and Fluorescence Spectra

Ensemble absorbance and photoluminescence spectra from QD–bioconjugate solutions were respectively acquired using a UV/visible spectrophotometer, Model 8453 (Agilent, CA) and a SPEX Fluorolog-2 fluorimeter (Horiba Jobin Yvon, Edison, New Jersey). Ensemble photoluminescence quantum yield were measured using Rhodamine B in ethanol

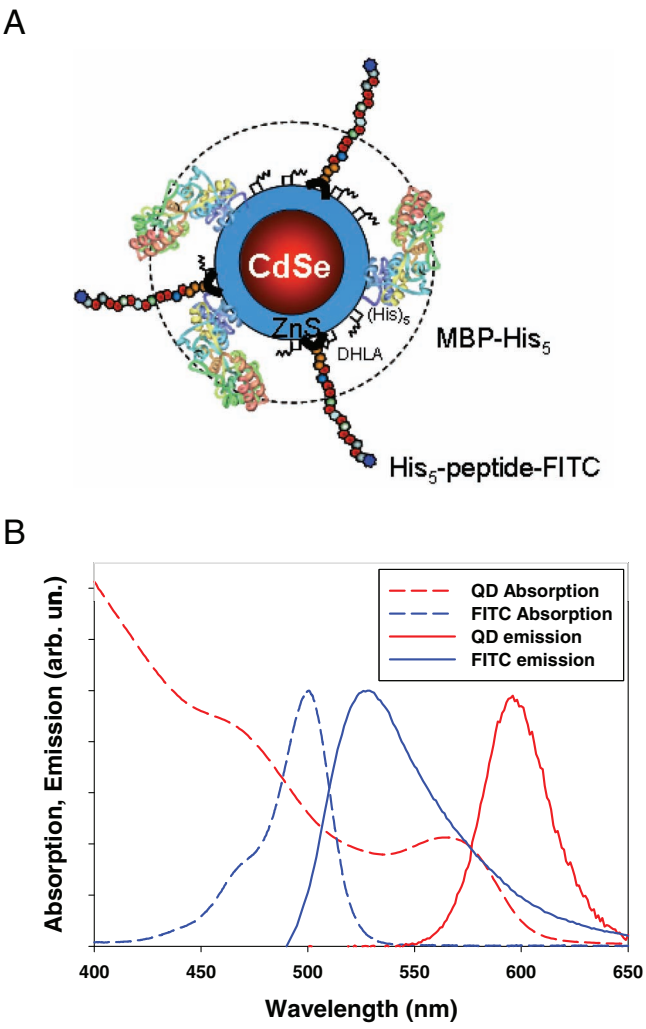

Figure 1. A) Schematics of a CdSe–ZnS core–shell QD capped with DHLA and simultaneously conjugated to MBP-His_5 and FITC-labeled peptide-His_5 (not to scale). B) The corresponding QD and dye absorption and emission spectra.

(PL QY = 70%) as a reference standard. The solutions were placed in a 10 mm optical path quartz cuvette (FUV, Spectrocell, Oreland, PA) for all data collection. Time-resolved QD PL decays were acquired using a homebuilt time-correlated single-photon counting (TCSPC) set-up equipped with a mode-locked tunable (from 920 to 710 nm) titanium sapphire laser source with a repetition rate of 80 MHz (Wideband Mai Tai, Newport Corp.), as previously described.[27] The 800 nm line was frequency-doubled (using a barium borate crystal, Photop Technologies) to provide a pulsed excitation line at 400 nm, which was used for all our experiments. Typical instrument response functions had a full width at half-maximum of 45 ps. Time-resolved QD PL decays were fitted using a three-exponential decay function.

$$PL(t) = a_1 e^{-t/\tau_1} + a_2 e^{-t/\tau_2} + a_3 e^{-t/\tau_{31}} + b \quad (1)$$

The exciton lifetime for the QD-MBP-His_5 conjugates were extracted using the weighted average, $\sum_i a_i \tau_i / \sum_i a_i$; a_1, a_2, a_3,

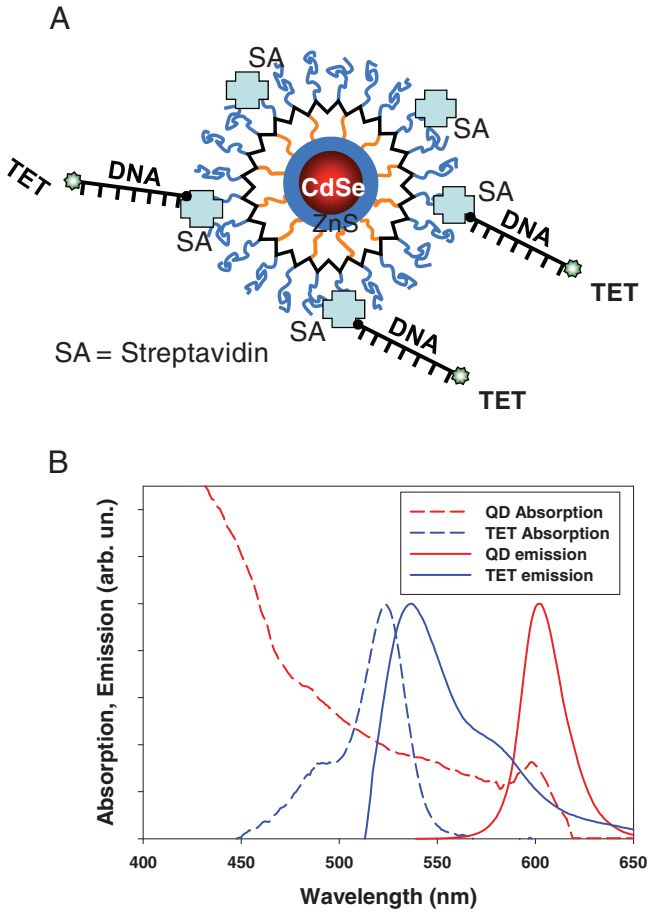

Figure 2. A) Schematics of a commercial SA-QD conjugated to TET-labeled single DNA strands (not to scale). B) The corresponding QD and dye absorption and emission spectra.

and b are constants. The ensemble quantum yield of QD-MBP-His_5 conjugates is proportional to this average exciton lifetime, assuming that the QD absorption cross-section and radiative rate remain constant (i.e., are not affected by the protein conjugation).[28]

2.4. Single QD FCA Measurements

Single QD colocalization measurements were performed on a Carl Zeiss Axiovert 200 confocal microscope, as previously described.[29,30] QD-conjugate stock solutions were prepared at 100 nM concentration. Prior to use the stock dispersion was diluted to ~1 nM, and a drop was placed on top of a glass coverslip at the focal plane of the microscope. A 488 nm excitation beam was focused through a 100×, 1.3 numerical aperture (NA) Fluar objective (Carl Zeiss) onto the sample, and the fluorescence signals from the QD and dye were collected through the same objective, passed through a dichroic mirror which removes contribution from the laser signal (515DCLP in conjugate configuration 1 or 540DCLP in conjugate configuration 2, Chroma, Rockingham, VT). Residual excitation signal was further discarded using a 488 nm notch filter (Kaiser Optical Systems, Ann Arbor, MI). The fluorescence signals from the QD and dye were further separated using a second dichroic filter/mirror (565DCXR in configuration 1 and 585DCLP in conjugate configuration 2, Chroma) and detected by two avalanche photodiodes (Perkin-Elmer, Fremont, CA). Time traces for both QD and dye signals were acquired with a 50 μs acquisition time in two runs for a total duration of 10 min, using a PCI 6602 acquisition board (National Instruments, Austin, TX) and a custom software written in Labview (National Instruments). The time-traces measured in each run consist of a series of signal bursts corresponding to the diffusion of a single QD-conjugate within the confocal volume, separated by periods with no detected signals.[17,30] This is important as it confirms that at the very low concentrations used, on average less than one QD–dye pair is present within the detection volume during the acquisition interval (bin), which in turn guarantees that the probability of detecting more than one QD–dye conjugate in a detection event is essentially negligible.

2.5. Single QD FCA Analysis

Analysis of the fluorescence traces was performed in Igor Pro (Wavemetrics), following the same procedures previously described.[30] Briefly, the fluorescence time traces were corrected to account for background contribution and spectral cross-talk using QD and fluorophore ensemble PL spectra. A threshold of 40 fluorescence counts was chosen to select fluorescence bursts with sufficient signal-to-noise ratio. The total number of such signal bursts in a single acquisition was generally ≥1000. Each burst was characterized by its emission ratio (Equation 2).

$$\eta = I_{QD}/(I_{QD} + I_f) \quad (2)$$

where I_f and I_{QD} represent the fluorophore and QD fluorescence intensities, respectively. Each sample was characterized by a histogram representing the fraction of fluorescence bursts exhibiting specific emission ratios.

2.6. FCS Measurements and Analysis

FCS measurements were carried out on the same set-up used for the FCA measurements, except that slightly higher QD concentrations (>100 nM) were needed in order to reduce the effects of background contribution. Autocorrelation of the fluorescence traces were then calculated post-acquisition from the acquired fluorescence time traces using Igor software. Autocorrelation traces were then fitted with either a simple diffusion model or included QD blinking. The diffusion model used the following theoretical autocorrelation function for a Brownian spherical object is

$$g_{2-diff}(\tau) \propto (1 + \tau/\tau_d)^{-1}(1 + (r_0^2/z_0^2)(\tau/\tau_d))^{-1/2} \quad (3)$$

where τ_d is a typical diffusion time, while r_0 and z_0 refer to the lateral and axial dimensions, respectively, of the Gaussian profile of the excitation beam.[31] Fluctuations

small NANO MICRO

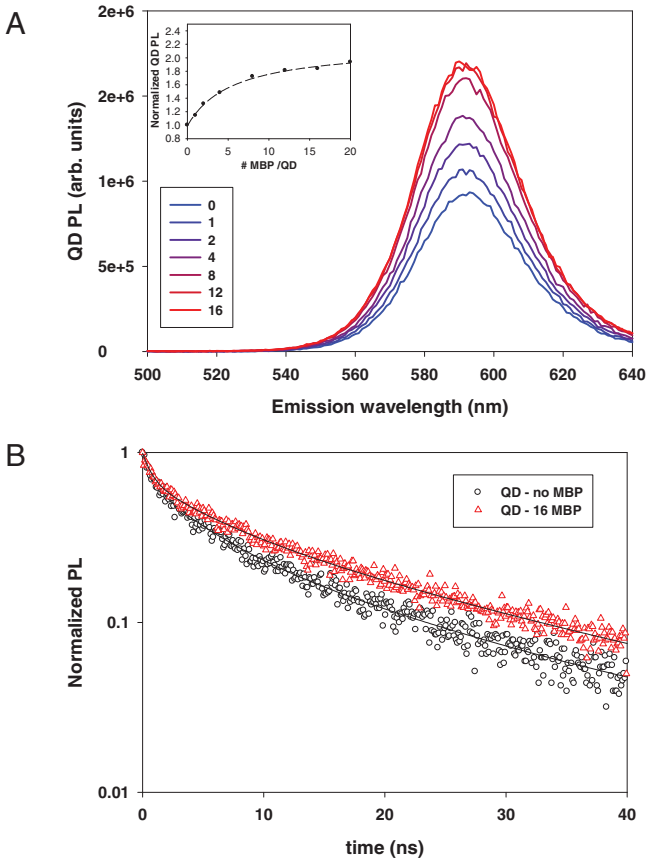

Figure 3. A) Normalized ensemble PL of DHLA-QD conjugated with different ratios of MBP to QD. B) Normalized ensemble time-resolved QD PL decay for 0 and 16 MBP:QD ratios.

attributed to the PL blinking of single QDs were taken into account by using a modified/corrected expression of the autocorrelation:

$$g_2(\tau) \propto g_{2-\mathrm{diff}}(\tau)(1 - B\tau^{2-m}) \quad (4)$$

where B is an experimental constant. In this analysis we assume that the probability density of blinking versus τ_{ON} and τ_{OFF} follows a power law decay with an exponent m: $P(\tau_{ON/OFF}) \propto (\tau_{ON/OFF})^{-m}$.[12,32]

3. Results

Figure 3 shows the steady-state fluorescence spectra for a set of DHLA-capped CdSe–ZnS QDs emitting at 590 nm dispersed in tetraborate buffer at pH 8.6. The PL QY measured for this sample was ~8–10%. Upon conjugation to MBP-His_5 a progressive increase in the QD emission with the conjugate valence takes place, with a QY of 0.2 measured at 16:1 MBP:QD. In addition, time-resolved PL data, shown in Figure 3B, indicate a slight lengthening of the excited states average lifetime for the QD–protein conjugates compared to DHLA-QDs.

For the fluorescence coincidence analysis, we prepared QDs conjugated to FITC-tagged peptides at a 3:1 average peptide-to-QD ratio. At this average ratio (valence), individually each QD is self-assembled with a few FITC-peptides (i.e., a negligible amount of unlabeled QDs is left in the solution). We know that heterogeneity in the conjugate valence (an inherent property of nanoparticle–bioconjugates) produces QD-assemblies that present discrete number of labeled peptides (0, 1, 2, 3, 4, 5…), and that the number follows a Poisson distribution. Thus, selecting an average valence of 3 essentially guarantees that no dye-free QDs will be left in the medium.[30] In addition, this dye-to-QD ratio was enough to produce strong and well-separated QD and dye signals, as it allowed us to compensate for the weaker extinction coefficient of the dye compared to that of the QD and produced measurable and spectrally well-separated PL peaks. This enabled the easy detection and discrimination between QD and FITC emissions for all QD-conjugates, independent of their individual QY. The QD-peptide-FITC assemblies were further conjugated to an increasing number of MBPs and their FCA traces were analyzed to obtain the corresponding emission ratio histograms; histograms for QDs with 0 and 16 MBP-His_5 are shown in **Figure 4**A. These histograms reflect the respective weights of the QD and FITC intensities in single fluorescence bursts, between $\eta = 0$, corresponding to fluorescence from the fluorophore only, and $\eta = 1$, corresponding to fluorescence from the QD only. All histograms exhibit two distinct peaks, centered at $\eta \approx 0$ and $\eta \approx 80\%$. When increasing the MBP:QD ratio, the positions of these peaks remain unchanged while their relative values vary. At a valence of 16 we measured an increase in the peak at $\eta = 80\%$ by a factor of ~4; conversely, the peak at $\eta = 0$ also decreased for QD-MBP/peptide-FITC conjugates.

Using our experimental conditions, we expect that all FITC-tagged peptides are conjugated to QDs.[21] Moreover, a solution of FITC-tagged peptides observed under identical conditions did not produce bursts above our detection threshold, due to the weak fluorescence of individual fluorescein dyes. We therefore attribute the peak at $\eta = 0$ in Figure 4A to "dark" QDs, exhibiting fluorescence from the conjugated fluorophores only when diffusing into the confocal observation volume. The second peak, around $\eta \approx 80\%$, is attributed to "bright" QDs, with simultaneous fluorescence contributions from the QD and the conjugated fluorophores. We thus associate the area under each of the two peaks to "dark" and "bright" QD population fractions, respectively. Figure 4B shows the increase of the "bright" fraction with increasing MBP:QD ratio, along with the corresponding increase in the total QD PL signal measured from FCA; the latter was evaluated from the sum of all QD fluorescence bursts in the time traces. We further define an average brightness per QD, calculated from the total QD PL divided by the number of fluorescence bursts in each sample. As shown in Figure 4B, the average brightness per QD stays constant for all MBP:QD ratios. The FCA data and the measured changes in the relative fraction of blinking QDs upon conjugation to the protein, is clearly correlated to the measured increase in the ensemble QY. We note that the measured bright fraction of QDs without any conjugated MBP is ~8%, which correlates well with the value of the ensemble QY.

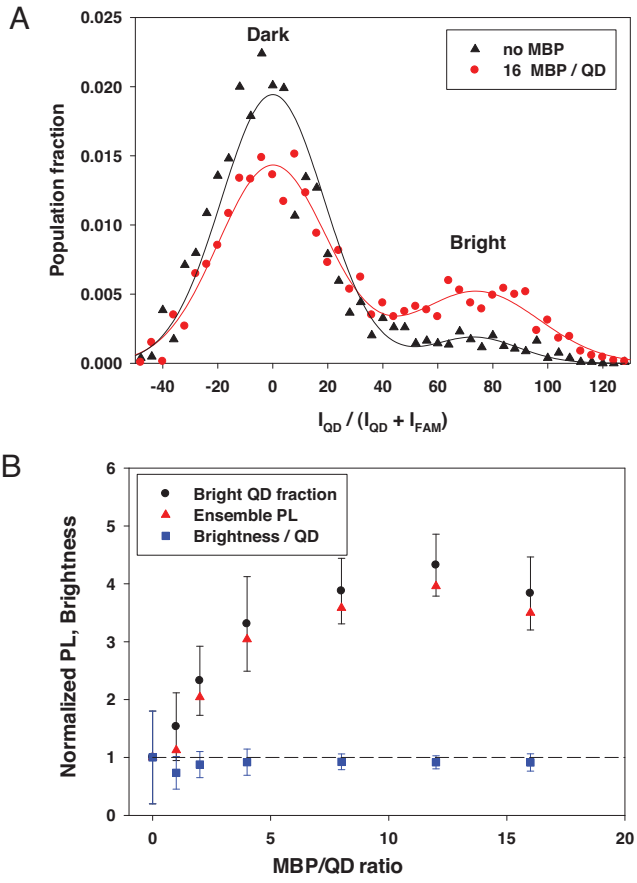

Figure 4. A) Emission ratio distributions obtained from single QD FCA for 0 (black, triangle) and 16 (red, circles) MBP:QD ratios and their corresponding fits. B) Normalized bright QD fraction, integrated PL, and brightness per QD obtained from single QD FCA measurements.

To investigate whether these results are specific to our DHLA surface chemistry or represent a general feature for all luminescent QDs, we examined commercially available QDs. These QDs were solubilized by encapsulation within an amphiphilic block copolymer, and functionalized with streptavidin groups (SA-QD, ~10 streptavidin per QD). To couple these QDs with organic dyes, we mixed SA-QDs with TET-labeled biotinylated DNA at an average of 10 TET–DNA per QD (Figure 2). At this ratio, QDs and TET yielded similar fluorescence intensities when excited at 488 nm. The obtained QDs have a ~40% ensemble QY. FCA measurements performed on this sample resulted in an emission histogram with 2 distinct populations. 85% of the fluorescence bursts have emission ratios around 70% (i.e., predominantly from the QD), with a second broad peak at low emission ratios (i.e., predominantly from the TET fluorophores), as shown in **Figure 5**.

Finally, we used fluorescence correlation spectroscopy (FCS) to investigate changes in DHLA QD photophysical properties when conjugated to MBP-His_5. A typical FCS curve is shown in **Figure 6**A. A simple Brownian diffusion model did not successfully fit the experimental autocorrelation functions. However, fits taking into account QD blinking and assuming that the probability densities follow

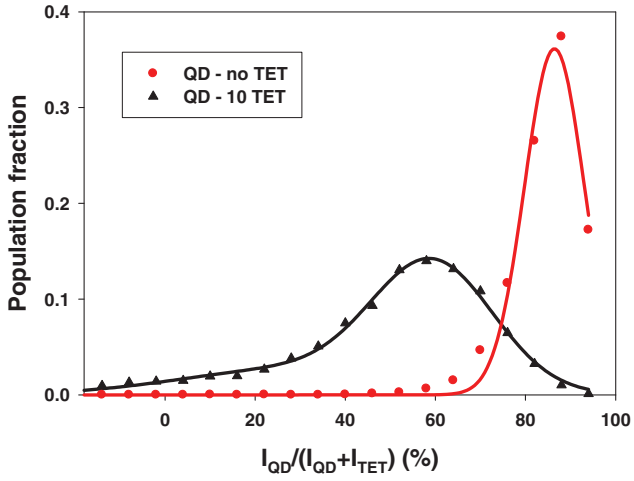

Figure 5. Emission ratio distribution obtained from single QD FCA for 0 (red, circles) and 10 (black, triangles) TET-DNA:QD ratios and their corresponding fits.

an inverse power law with τ, $P(\tau_{ON/OFF}) \propto (\tau_{ON/OFF})^{-m}$ with exponent m = 1.6–1.7, were in much better agreements with the data.[12,33] Since diffusion processes are slower than millisecond timescales and the QD photobleaching was negligible for our system, we assumed that the main source for fluctuations below the millisecond range was dominated by QD blinking; we used the initial decay slope of the FCS curve at $\tau = 100$ µs as a signature of blinking fluctuations. The obtained slopes of the QD FCS decay curves measured in the absence and presence of MBP-His_5 proteins are reported in Figure 6B, at different excitation intensities. We observed in both cases an increase in the FCS decay slope with increasing excitation power. This is consistent with previously reported faster blinking dynamics with increasing excitation power.[14] However, no differences were observed between QD samples in the presence or absence of proteins.

4. Discussion

The steady state and time-resolved fluorescence data in Figure 3 show that when the QD-MBP-His_5 conjugate valence is increased from 1 to saturation, the PL emission is increased by a factor of ~2. This result confirms prior findings which show that when His-appended proteins are self-assembled onto DHLA-capped QDs, the PL yield is progressively enhanced before reaching saturation at the maximum packing allowed by steric considerations.[18,19] The data also show that the PL enhancement is further accompanied by a slight lengthening in the exciton lifetime, indicative of a small decrease in the nonradiative rates. Assuming that the QD absorption cross-section and radiative rate do not change upon self-assembly with MBP-His_5, we can estimate the change in QD PL quantum yield from the fluorescence lifetime data. However, the measured change in the exciton lifetime can account only for a ~19% difference in QY between the two sets of solutions; this is much smaller than the ~100% increase obtained from steady-state measurements

small NANO MICRO

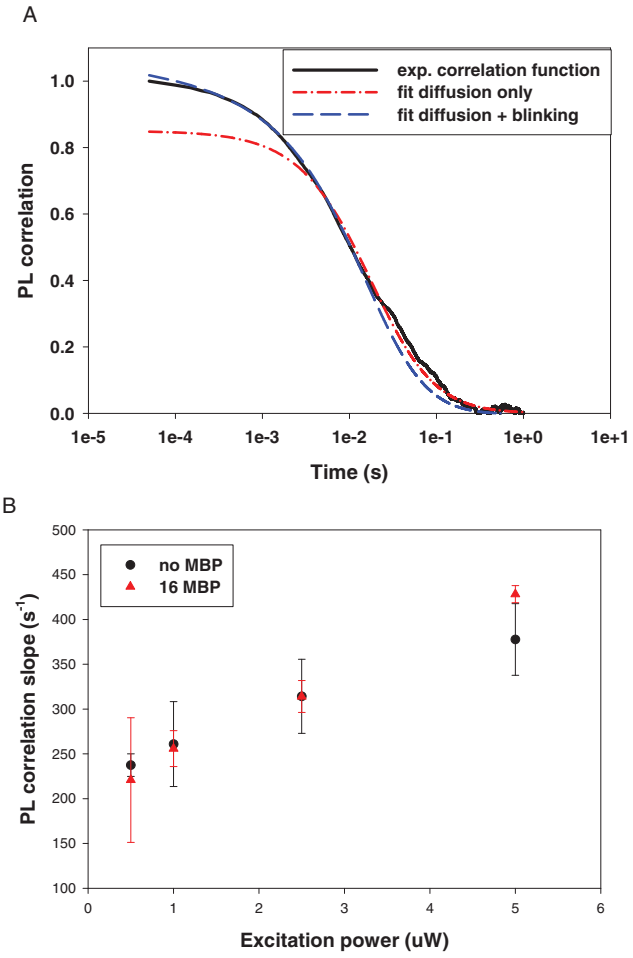

Figure 6. A) FCS measurements of a DHLA-QD solution: experimental curve (solid, black), theoretical fit for diffusion fluctuations only (dashed-dotted, red), and theoretical fit for diffusion and blinking fluctuations (dashed, blue). B) Evolution of the PL correlation slope as a function of excitation power for DHLA QDs for 0 (black circles) and 16 (red triangles) self-assembled MBP-His_5 per QD.

shown in Figure 3A. This indicates that the enhancement in the ensemble fluorescence QY cannot be simply attributed to an increase in the PL yield of individual QDs. We instead attribute it to an increase in the fraction of emitting, or "bright" QDs in the sample.

The FCA data shown in Figure 4 support this model, and can be interpreted within the framework of a fluorescence emission generated from a mixture of two sets of QDs in the solution. One fraction is "bright"—though these QDs emit intermittently, while the other is non-emitting ("permanently dark"). The macroscopic PL yield reflects the relative fraction of "bright" versus "dark" QD populations. This idea was first proposed by Webb and co-workers, and our set of data fully agrees with that rationale and the results reported in reference [17]. The increase in the ensemble QY measured for solution of QD-MBP conjugates shown in Figure 3 supports (at least partially) the single-molecule data where the fraction of bright QDs was increased by ~4. The constant position of the "bright QD" peak at $\eta \approx 80\%$ in Figure 4A is also consistent with this model. In contrast, a homogeneous increase in the individual QD QYs would produce a shift in this peak location towards higher emission ratios, as anticipated from Equation 2; it should also be accompanied with a sizable change in the exciton lifetime. Conversely, the SA-QDs have relatively high ensemble QYs, and they do not experience a change in their emission when coupled to a few DNA molecules. The FCA data showed only two peaks at distinct η values; only one ratio of QD:dye conjugates was used. The high ensemble QY in this QD sample is reflected by a large "bright" fraction (85%), similar to what was reported by Webb's group.

The fact that the bright fraction of QDs in the first sample configuration can be modified upon self-assembly with a His-tagged protein helps shed some light on the nature of the two species of QDs. The decrease in the dark QD fraction with increasing protein:QD ratios suggests that the non-emitting state of the dark QD is at least partially reversible, and is not caused by irreversible structural defects. It must originate from surface defects, such as incomplete surface passivation and charge trapping, resulting in fast nonradiative exciton recombination. Such recombination pathway may indeed be fast enough to completely eliminate PL emission from a QD, making it effectively dark. Protein self-assembly directly onto the QD surface could improve the surface passivation, reducing the effects of nonradiative recombination and increasing the fraction of emitting QDs in the sample. However, our experiments cannot determine the time scale of the dark state, and whether or not QDs slowly switch back and forth between these two subpopulations. In addition, other distinct phenomena are susceptible to switch the QDs between bright and dark states, such as slow blinking, in which a QD becomes transiently dark due to photo-induced charging. Our FCS results suggest that fast QD blinking dynamics is not affected by surface assembly of His-tagged proteins. Consequently, it seems unlikely that changes in QD blinking behavior causes the relative change in the apparent QD "bright" and "dark" fractions; however a more detailed study on longer time scales would be necessary to confirm this. Finally, we note that the solution phase PL enhancement upon self-assembly with proteins (×2 at the highest valence) is correlated but not commensurate with the one measured with FCA (×4 at the highest valence). This discrepancy may originate from the differences in observation conditions, and in particular in the excitation intensity used, which is much higher for single QD FCA than for ensemble measurements. This, in turn, will likely affect the apparent QD QY due to photo-induced effects (e.g., increase in blinking rates, photo-brightening). This emphasizes that the notion of QD PL quantum yield should be used with care, since this value appears to be highly heterogeneous in a QD population, and may also be dependent upon excitation conditions.

5. Conclusion

We have investigated the correlation between solution-phase (ensemble) quantum yield of dispersions of CdSe–ZnS QDs and the fluorescence emission of individual QDs. For this we exploited the enhancement in the macroscopic quantum yield of water-soluble QDs capped with dihydrolipoic acid upon self-assembly with polyhistidine-appended proteins, and probed the effects of that increase on the fluorescence emission

of single QD conjugates under continuous laser irradiation. We used fluorescence coincidence analysis to detect the presence of "bright" and "dark" single QDs and tracked the change in their relative fractions as the QD–conjugate valence was varied. Our study clearly showed that in a QD dispersion, there exists two QD populations, one that is "permanently" dark while the other fluoresces. A change in the yield of the solution arises from changes in the relative fraction of the two QD species, with a higher fraction of single emitting QDs measured for higher yields, and vice versa. The above correlation between macroscopic yield and fraction of "bright" QDs is not accompanied by change in the average brightness of single QDs; the latter stays constant at all QYs. FCS measurements showed no change in the blinking dynamics of single QDs upon conjugation to proteins, which indicates that higher yields do not result from changes in the blinking properties of individual nanocrystals. These findings support the rationale that a dispersion of fluorescing nanocrystals is made of a mixture of fixed-brightness emitting QDs and "dark" QDs, and it is the relative ratio of the two species that is changed when the macroscopic PL yield of the solution is altered. Nonetheless, we found that the increase in the fraction of bright QDs in a sample was larger by a factor of 2 than the enhancement in macroscopic PL yield.

Acknowledgements

The authors acknowledge NRL, ONR, and DTRA for financial support. DF acknowledges the NRC postdoctoral fellowship.

This Full Paper is part of the Special Issue dedicated to Chad Mirkin in celebration of 20 years of influential research at Northwestern University.

[1] S. V. Gaponenko, U. Woggon, in *Optical Properties of Semiconductor Nanostructures* (Ed: C. Klingshirn), Springer-Verlag, Berlin **2004**, 284.
[2] *Nanocrystal Quantum Dots*, 2nd ed. (Ed: V. I. Klimov), Taylor and Francis, London **2010**.
[3] C. B. Murray, D. J. Norris, M. G. Bawendi, *J. Am. Chem. Soc.* **1993**, *115*, 8706.
[4] C.R. Bullen, P. Mulvaney, *Nano Lett.* **2004**, *4*, 2303.
[5] J. Park, J. Joo, S. G. Kwon, Y. Jang, T. Hyeon, *Angew. Chem. Int. Ed.* **2007**, *46*, 4630.
[6] Z. A. Peng, X. G. Peng, *J. Am. Chem. Soc.* **2001**, *123*, 183.
[7] L. H. Qu, Z. A. Peng, X. G. Peng, *Nano Lett.* **2001**, *1*, 333.
[8] W. W. Yu, X. G. Peng, *Angew. Chem. Int. Ed.* **2002**, *41*, 2368.
[9] B. O. Dabbousi, J. RodriguezViejo, F. V. Mikulec, J. R. Heine, H. Mattoussi, R. Ober, K. F. Jensen, M. G. Bawendi, *J. Phys. Chem. B* **1997**, *101*, 9463.
[10] M. A. Hines, P. Guyot-Sionnest, *J. Phys. Chem.-Us* **1996**, *100*, 468.
[11] M. Nirmal, B. O. Dabbousi, M. G. Bawendi, J. J. Macklin, J. K. Trautman, T. D. Harris, L. E. Brus, *Nature* **1996**, *383*, 802.
[12] M. Kuno, D. P. Fromm, H. F. Hamann, A. Gallagher, D. J. Nesbitt, *J. Chem. Phys.* **2001**, *115*, 1028.
[13] A. L. Efros, M. Rosen, *Phys. Rev. Lett* **1997**, *78*, 1110.
[14] K. T. Shimizu, R. G. Neuhauser, C. A. Leatherdale, S. A. Empedocles, W. K. Woo, M. G. Bawendi, *Phys. Rev. B* **2001**, *6320*, 205316.
[15] D. E. Gomez, J. van Embden, J. Jasieniak, T. A. Smith, P. Mulvaney, *Small* **2006**, *2*, 204.
[16] M. Kuno, D. P. Fromm, S. T. Johnson, A. Gallagher, D. J. Nesbitt, *Phys. Rev. B* **2003**, *67*, 125304.
[17] J. Yao, D. R. Larson, H. D. Vishwasrao, W. R. Zipfel, W. W. Webb, *Proc. Natl. Acad. Sci. USA* **2005**, *102*, 14284.
[18] I. L. Medintz, A. R. Clapp, H. Mattoussi, E. R. Goldman, B. Fisher, J. M. Mauro, *Nat. Mater.* **2003**, *2*, 630.
[19] H. Mattoussi, J. M. Mauro, E. R. Goldman, G. P. Anderson, V. C. Sundar, F. V. Mikulec, M. G. Bawendi, *J. Am. Chem. Soc.* **2000**, *122*, 12142.
[20] A. R. Clapp, E. R. Goldman, H. Mattoussi, *Nat. Protoc.* **2006**, *1*, 1258.
[21] K. E. Sapsford, T. Pons, I. L. Medintz, S. Higashiya, F. M. Brunel, P. E. Dawson, H. Mattoussi, *J. Phys. Chem. C* **2007**, *111*, 11528.
[22] A. M. Dennis, D. C. Sotto, B. C. Mei, I. L. Medintz, H. Mattoussi, G. Bao, *Bioconjugate Chem.* **2010**, *21*, 1160.
[23] W. Liu, M. Howarth, A. B. Greytak, Y. Zheng, D. G. Nocera, A. Y. Ting, M. G. Bawendi, *J. Am. Chem. Soc.* **2008**, *130*, 1274.
[24] W. C. Chan, P. D. White, *Fmoc Solid Phase Peptide Synthesis: A Practical Approach*, Oxford University Press, New York **2000**.
[25] G. T. Hermanson, *Bioconjugate Techniques*, Academic Press, San Diego **1996**.
[26] K. E. Sapsford, D. Farrell, S. Steven Sun, A. Rasooly, H. Mattoussi, I. L. Medintz, *Sens. Actuators B: Chem.* **2009**, *139*, 13.
[27] A. F. Grimes, S. E. Call, D. A. Vicente, D. S. English, E. J. Harbron, *J. Phys. Chem. B* **2006**, *110*, 19183.
[28] J. R. Lakowicz, *Principles of Fluorescence Spectroscopy*, 2nd ed., Kluwer Academic, New York **1999**.
[29] M. A. Morgan, K. Okamoto, J. D. Kahn, D. S. English, *Biophys. J.* **2005**, *89*, 2588.
[30] T. Pons, I. L. Medintz, X. Wang, D. S. English, H. Mattoussi, *J. Am. Chem. Soc.* **2006**, *128*, 15324.
[31] E. Haustein, P. Schwille, *Methods* **2003**, *29*, 153.
[32] R. Verberk, A. M. van Oijen, M. Orrit, *Phys. Rev. B* **2002**, *66*, 233202.
[33] I. H. Chung, M. G. Bawendi, *Phys. Rev. B* **2004**, *70*, 165304.

Received: April 26, 2011
Published online: June 28, 2011

